



## Search for $WH$ associated production in $5.3 \text{ fb}^{-1}$ of $p\bar{p}$ collisions at the Fermilab Tevatron

D0 Collaboration

V.M. Abazov<sup>ak</sup>, B. Abbott<sup>bw</sup>, B.S. Acharya<sup>ae</sup>, M. Adams<sup>ay</sup>, T. Adams<sup>aw</sup>, G.D. Alexeev<sup>ak</sup>, G. Alkhazov<sup>ao</sup>, A. Alton<sup>bk,1</sup>, G. Alverson<sup>bj</sup>, G.A. Alves<sup>b</sup>, L.S. Ancu<sup>aj</sup>, M. Aoki<sup>ax</sup>, M. Arov<sup>bh</sup>, A. Askew<sup>aw</sup>, B. Åsman<sup>ap,aq</sup>, O. Atramentov<sup>bo</sup>, C. Avila<sup>i</sup>, J. BackusMayer<sup>cd</sup>, F. Badaud<sup>n</sup>, L. Bagby<sup>ax</sup>, B. Baldin<sup>ax</sup>, D.V. Bandurin<sup>aw</sup>, S. Banerjee<sup>ae</sup>, E. Barberis<sup>bj</sup>, P. Baringer<sup>bf</sup>, J. Barreto<sup>c</sup>, J.F. Bartlett<sup>ax</sup>, U. Bassler<sup>s</sup>, V. Bazterra<sup>ay</sup>, S. Beale<sup>f,g</sup>, A. Bean<sup>bf</sup>, M. Begalli<sup>c</sup>, M. Begel<sup>bu</sup>, C. Belanger-Champagne<sup>ap,aq</sup>, L. Bellantoni<sup>ax</sup>, S.B. Beri<sup>ac</sup>, G. Bernardi<sup>r</sup>, R. Bernhard<sup>x</sup>, I. Bertram<sup>ar</sup>, M. Besançon<sup>s</sup>, R. Beuselinck<sup>as</sup>, V.A. Bezzubov<sup>an</sup>, P.C. Bhat<sup>ax</sup>, V. Bhatnagar<sup>ac</sup>, G. Blazey<sup>az</sup>, S. Blessing<sup>aw</sup>, K. Bloom<sup>bn</sup>, A. Boehnlein<sup>ax</sup>, D. Boline<sup>bt</sup>, T.A. Bolton<sup>bg</sup>, E.E. Boos<sup>am</sup>, G. Borissov<sup>ar</sup>, T. Bose<sup>bi</sup>, A. Brandt<sup>bz</sup>, O. Brandt<sup>y</sup>, R. Brock<sup>bl</sup>, G. Brooijmans<sup>br</sup>, A. Bross<sup>ax</sup>, D. Brown<sup>r</sup>, J. Brown<sup>r</sup>, X.B. Bu<sup>ax</sup>, M. Buehler<sup>cc</sup>, V. Buescher<sup>z</sup>, V. Bunichev<sup>am</sup>, S. Burdin<sup>ar,2</sup>, T.H. Burnett<sup>cd</sup>, C.P. Buszello<sup>ap,aq</sup>, B. Calpas<sup>p</sup>, E. Camacho-Pérez<sup>ah</sup>, M.A. Carrasco-Lizarraga<sup>bf</sup>, B.C.K. Casey<sup>ax</sup>, H. Castilla-Valdez<sup>ah</sup>, S. Chakrabarti<sup>bt</sup>, D. Chakraborty<sup>az</sup>, K.M. Chan<sup>bd</sup>, A. Chandra<sup>cb</sup>, G. Chen<sup>bf</sup>, S. Chevalier-Théry<sup>s</sup>, D.K. Cho<sup>by</sup>, S.W. Cho<sup>ag</sup>, S. Choi<sup>ag</sup>, B. Choudhary<sup>ad</sup>, T. Christoudias<sup>as</sup>, S. Cihangir<sup>ax</sup>, D. Claes<sup>bn</sup>, J. Clutter<sup>bf</sup>, M. Cooke<sup>ax</sup>, W.E. Cooper<sup>ax</sup>, M. Corcoran<sup>cb</sup>, F. Couderc<sup>s</sup>, M.-C. Cousinou<sup>p</sup>, A. Croc<sup>s</sup>, D. Cutts<sup>by</sup>, A. Das<sup>au</sup>, G. Davies<sup>as</sup>, K. De<sup>bz</sup>, S.J. de Jong<sup>aj</sup>, E. De La Cruz-Burelo<sup>ah</sup>, F. Déliot<sup>s</sup>, M. Demarteau<sup>ax</sup>, R. Demina<sup>bs</sup>, D. Denisov<sup>ax</sup>, S.P. Denisov<sup>an</sup>, S. Desai<sup>ax</sup>, K. DeVaughan<sup>bn</sup>, H.T. Diehl<sup>ax</sup>, M. Diesburg<sup>ax</sup>, A. Dominguez<sup>bn</sup>, T. Dorland<sup>cd</sup>, A. Dubey<sup>ad</sup>, L.V. Dudko<sup>am</sup>, D. Duggan<sup>bo</sup>, A. Duperrin<sup>p</sup>, S. Dutt<sup>ac</sup>, A. Dyshkant<sup>az</sup>, M. Eads<sup>bn</sup>, D. Edmunds<sup>bl</sup>, J. Ellison<sup>av</sup>, V.D. Elvira<sup>ax</sup>, Y. Enari<sup>r</sup>, H. Evans<sup>bb</sup>, A. Evdokimov<sup>bu</sup>, V.N. Evdokimov<sup>an</sup>, G. Facini<sup>bj</sup>, T. Ferbel<sup>bs</sup>, F. Fiedler<sup>z</sup>, F. Filthaut<sup>aj</sup>, W. Fisher<sup>bl</sup>, H.E. Fisk<sup>ax</sup>, M. Fortner<sup>az</sup>, H. Fox<sup>ar</sup>, S. Fuess<sup>ax</sup>, T. Gadfort<sup>bu</sup>, A. Garcia-Bellido<sup>bs</sup>, V. Gavrilov<sup>al</sup>, P. Gay<sup>n</sup>, W. Geist<sup>t</sup>, W. Geng<sup>p,bl</sup>, D. Gerbaudo<sup>bp</sup>, C.E. Gerber<sup>ay</sup>, Y. Gershtein<sup>bo</sup>, G. Ginther<sup>ax,bs</sup>, G. Golovanov<sup>ak</sup>, A. Goussiou<sup>cd</sup>, P.D. Grannis<sup>bt</sup>, S. Greder<sup>t</sup>, H. Greenlee<sup>ax</sup>, Z.D. Greenwood<sup>bh</sup>, E.M. Gregores<sup>d</sup>, G. Grenier<sup>u,v</sup>, Ph. Gris<sup>n</sup>, J.-F. Grivaz<sup>q</sup>, A. Grohsjean<sup>s</sup>, S. Grünendahl<sup>ax</sup>, M.W. Grünewald<sup>af</sup>, F. Guo<sup>bt</sup>, G. Gutierrez<sup>ax</sup>, P. Gutierrez<sup>bw</sup>, A. Haas<sup>br,3</sup>, S. Hagopian<sup>aw</sup>, J. Haley<sup>bj</sup>, L. Han<sup>h</sup>, K. Harder<sup>at</sup>, A. Harel<sup>bs</sup>, J.M. Hauptman<sup>be</sup>, J. Hays<sup>as</sup>, T. Head<sup>at</sup>, T. Hebbeker<sup>w</sup>, D. Hedin<sup>az</sup>, H. Hegab<sup>bx</sup>, A.P. Heinson<sup>av</sup>, U. Heintz<sup>by</sup>, C. Hensel<sup>y</sup>, I. Heredia-De La Cruz<sup>ah</sup>, K. Herner<sup>bk</sup>, M.D. Hildreth<sup>bd</sup>, R. Hirosky<sup>cc</sup>, T. Hoang<sup>aw</sup>, J.D. Hobbs<sup>bt</sup>, B. Hoeneisen<sup>m</sup>, M. Hohlfield<sup>z</sup>, S. Hossain<sup>bw</sup>, Z. Hubacek<sup>k,s</sup>, N. Huske<sup>r</sup>, V. Hynek<sup>k</sup>, I. Iashvili<sup>bq</sup>, R. Illingworth<sup>ax</sup>, A.S. Ito<sup>ax</sup>, S. Jabeen<sup>by</sup>, M. Jaffré<sup>q</sup>, S. Jain<sup>bq</sup>, D. Jamin<sup>p</sup>, R. Jesik<sup>as</sup>, K. Johns<sup>au</sup>, M. Johnson<sup>ax</sup>, D. Johnston<sup>bn</sup>, A. Jonckheere<sup>ax</sup>, P. Jonsson<sup>as</sup>, J. Joshi<sup>ac</sup>, A. Juste<sup>ax,4</sup>, K. Kaadze<sup>bg</sup>, E. Kajfasz<sup>p</sup>, D. Karmanov<sup>am</sup>, P.A. Kasper<sup>ax</sup>, I. Katsanos<sup>bn</sup>, R. Kehoe<sup>ca</sup>, S. Kermiche<sup>p</sup>, N. Khalatyan<sup>ax</sup>, A. Khanov<sup>bx</sup>, A. Kharchilava<sup>bq</sup>, Y.N. Kharzheev<sup>ak</sup>, D. Khatidze<sup>by</sup>, M.H. Kirby<sup>ba</sup>, J.M. Kohli<sup>ac</sup>, A.V. Kozelov<sup>an</sup>, J. Kraus<sup>bl</sup>, A. Kumar<sup>bq</sup>, A. Kupco<sup>l</sup>, T. Kurča<sup>u,v</sup>, V.A. Kuzmin<sup>am</sup>, J. Kvita<sup>j</sup>, S. Lammers<sup>bb</sup>, G. Landsberg<sup>by</sup>, P. Lebrun<sup>u,v</sup>, H.S. Lee<sup>ag</sup>, S.W. Lee<sup>be</sup>, W.M. Lee<sup>ax</sup>, J. Lellouch<sup>r</sup>, L. Li<sup>av</sup>, Q.Z. Li<sup>ax</sup>, S.M. Lietti<sup>e</sup>, J.K. Lim<sup>ag</sup>, D. Lincoln<sup>ax</sup>, J. Linnemann<sup>bl</sup>, V.V. Lipaev<sup>an</sup>, R. Lipton<sup>ax</sup>, Y. Liu<sup>h</sup>, Z. Liu<sup>f,g</sup>, A. Lobodenko<sup>ao</sup>, M. Lokajicek<sup>l</sup>, P. Love<sup>ar</sup>, H.J. Lubatti<sup>cd</sup>, R. Luna-Garcia<sup>ah,5</sup>, A.L. Lyon<sup>ax</sup>, A.K.A. Maciel<sup>b</sup>, D. Mackin<sup>cb</sup>, R. Madar<sup>s</sup>, R. Magaña-Villalba<sup>ah</sup>, S. Malik<sup>bn</sup>, V.L. Malyshev<sup>ak</sup>, Y. Maravin<sup>bg</sup>, J. Martínez-Ortega<sup>ah</sup>, R. McCarthy<sup>bt</sup>, C.L. McGivern<sup>bf</sup>, M.M. Meijer<sup>aj</sup>, A. Melnitchouk<sup>bm</sup>, D. Menezes<sup>az</sup>, P.G. Mercadante<sup>d</sup>, M. Merkin<sup>am</sup>, A. Meyer<sup>w</sup>, J. Meyer<sup>y</sup>, F. Miconi<sup>t</sup>, N.K. Mondal<sup>ae</sup>, G.S. Muanza<sup>p</sup>,

M. Mulhearn<sup>cc</sup>, E. Nagy<sup>p</sup>, M. Naimuddin<sup>ad</sup>, M. Narain<sup>by</sup>, R. Nayyar<sup>ad</sup>, H.A. Neal<sup>bk</sup>, J.P. Negret<sup>i</sup>, P. Neustroev<sup>ao</sup>, S.F. Novaes<sup>e</sup>, T. Nunnemann<sup>aa</sup>, G. Obrant<sup>ao</sup>, J. Orduna<sup>ah</sup>, N. Osman<sup>as</sup>, J. Osta<sup>bd</sup>, G.J. Otero y Garzón<sup>a</sup>, M. Owen<sup>at</sup>, M. Padilla<sup>av</sup>, M. Pangilinan<sup>by</sup>, N. Parashar<sup>bc</sup>, V. Parihar<sup>by</sup>, S.K. Park<sup>ag</sup>, J. Parsons<sup>br</sup>, R. Partridge<sup>by,3</sup>, N. Parua<sup>bb</sup>, A. Patwa<sup>bu</sup>, B. Penning<sup>ax</sup>, M. Perfilov<sup>am</sup>, K. Peters<sup>at</sup>, Y. Peters<sup>at</sup>, G. Petrillo<sup>bs</sup>, P. Pétrouff<sup>q</sup>, R. Piegaia<sup>a</sup>, J. Piper<sup>bl</sup>, M.-A. Pleier<sup>bu</sup>, P.L.M. Podesta-Lerma<sup>ah,6</sup>, V.M. Podstavkov<sup>ax</sup>, M.-E. Pol<sup>b</sup>, P. Polozov<sup>al</sup>, A.V. Popov<sup>an</sup>, M. Prewitt<sup>cb</sup>, D. Price<sup>bb</sup>, S. Protopopescu<sup>bu</sup>, J. Qian<sup>bk</sup>, A. Quadt<sup>y</sup>, B. Quinn<sup>bm</sup>, M.S. Rangel<sup>b</sup>, K. Ranjan<sup>ad</sup>, P.N. Ratoff<sup>ar</sup>, I. Razumov<sup>an</sup>, P. Renkel<sup>ca</sup>, M. Rijssenbeek<sup>bt</sup>, I. Ripp-Baudot<sup>t</sup>, F. Rizatdinova<sup>bx</sup>, M. Rominsky<sup>ax</sup>, C. Royon<sup>s</sup>, P. Rubinov<sup>ax</sup>, R. Ruchti<sup>bd</sup>, G. Safronov<sup>al</sup>, G. Sajot<sup>o</sup>, A. Sánchez-Hernández<sup>ah</sup>, M.P. Sanders<sup>aa</sup>, B. Sanghi<sup>ax</sup>, A.S. Santos<sup>e</sup>, G. Savage<sup>ax</sup>, L. Sawyer<sup>bh</sup>, T. Scanlon<sup>as</sup>, R.D. Schamberger<sup>bt</sup>, Y. Scheglov<sup>ao</sup>, H. Schellman<sup>ba</sup>, T. Schliephake<sup>ab</sup>, S. Schlobohm<sup>cd</sup>, C. Schwanenberger<sup>at</sup>, R. Schwienhorst<sup>bl</sup>, J. Sekaric<sup>bf</sup>, H. Severini<sup>bw</sup>, E. Shabalina<sup>y</sup>, V. Shary<sup>s</sup>, A.A. Shchukin<sup>an</sup>, R.K. Shivpuri<sup>ad</sup>, V. Simak<sup>k</sup>, V. Sirotenko<sup>ax</sup>, P. Skubic<sup>bw</sup>, P. Slattery<sup>bs</sup>, D. Smirnov<sup>bd</sup>, K.J. Smith<sup>bq</sup>, G.R. Snow<sup>bn</sup>, J. Snow<sup>bv</sup>, S. Snyder<sup>bu</sup>, S. Söldner-Rembold<sup>at</sup>, L. Sonnenschein<sup>w</sup>, A. Sopczak<sup>ar</sup>, M. Sosebee<sup>bz</sup>, K. Soustruznik<sup>j</sup>, B. Spurlock<sup>bz</sup>, J. Stark<sup>o</sup>, V. Stolin<sup>al</sup>, D.A. Stoyanova<sup>an</sup>, M. Strauss<sup>bw</sup>, D. Strom<sup>ay</sup>, L. Stutte<sup>ax</sup>, L. Suter<sup>at</sup>, P. Svoisky<sup>bw</sup>, M. Takahashi<sup>at</sup>, A. Tanasijczuk<sup>a</sup>, W. Taylor<sup>f,g</sup>, M. Titov<sup>s</sup>, V.V. Tokmenin<sup>ak</sup>, Y.-T. Tsai<sup>bs</sup>, D. Tsybychev<sup>bt</sup>, B. Tuchming<sup>s</sup>, C. Tully<sup>bp</sup>, P.M. Tuts<sup>br</sup>, L. Uvarov<sup>ao</sup>, S. Uvarov<sup>ao</sup>, S. Uzunyan<sup>az</sup>, R. Van Kooten<sup>bb</sup>, W.M. van Leeuwen<sup>ai</sup>, N. Varelas<sup>ay</sup>, E.W. Varnes<sup>au</sup>, I.A. Vasilyev<sup>an</sup>, P. Verdier<sup>u,v</sup>, L.S. Vertogradov<sup>ak</sup>, M. Verzocchi<sup>ax</sup>, M. Vesterinen<sup>at</sup>, D. Vilanova<sup>s</sup>, P. Vint<sup>as</sup>, P. Vokac<sup>k</sup>, H.D. Wahl<sup>aw</sup>, M.H.L.S. Wang<sup>bs</sup>, J. Warchol<sup>bd</sup>, G. Watts<sup>cd</sup>, M. Wayne<sup>bd</sup>, M. Weber<sup>ax,7</sup>, L. Welty-Rieger<sup>ba</sup>, A. White<sup>bz</sup>, D. Wicke<sup>ab</sup>, M.R.J. Williams<sup>ar</sup>, G.W. Wilson<sup>bf</sup>, S.J. Wimpenny<sup>av</sup>, M. Wobisch<sup>bh</sup>, D.R. Wood<sup>bj</sup>, T.R. Wyatt<sup>at</sup>, Y. Xie<sup>ax</sup>, C. Xu<sup>bk</sup>, S. Yacoob<sup>ba</sup>, R. Yamada<sup>ax</sup>, W.-C. Yang<sup>at</sup>, T. Yasuda<sup>ax</sup>, Y.A. Yatsunenkov<sup>ak</sup>, Z. Ye<sup>ax</sup>, H. Yin<sup>ax</sup>, K. Yip<sup>bu</sup>, S.W. Youn<sup>ax</sup>, J. Yu<sup>bz</sup>, S. Zelitch<sup>cc</sup>, T. Zhao<sup>cd</sup>, B. Zhou<sup>bk</sup>, J. Zhu<sup>bk</sup>, M. Zielinski<sup>bs</sup>, D. Zieminska<sup>bb</sup>, L. Zivkovic<sup>by</sup>

<sup>a</sup> Universidad de Buenos Aires, Buenos Aires, Argentina<sup>b</sup> LAFEX, Centro Brasileiro de Pesquisas Físicas, Rio de Janeiro, Brazil<sup>c</sup> Universidade do Estado do Rio de Janeiro, Rio de Janeiro, Brazil<sup>d</sup> Universidade Federal do ABC, Santo André, Brazil<sup>e</sup> Instituto de Física Teórica, Universidade Estadual Paulista, São Paulo, Brazil<sup>f</sup> Simon Fraser University, Vancouver, British Columbia, Canada<sup>g</sup> York University, Toronto, Ontario, Canada<sup>h</sup> University of Science and Technology of China, Hefei, People's Republic of China<sup>i</sup> Universidad de los Andes, Bogotá, Colombia<sup>j</sup> Charles University, Faculty of Mathematics and Physics, Center for Particle Physics, Prague, Czech Republic<sup>k</sup> Czech Technical University in Prague, Prague, Czech Republic<sup>l</sup> Center for Particle Physics, Institute of Physics, Academy of Sciences of the Czech Republic, Prague, Czech Republic<sup>m</sup> Universidad San Francisco de Quito, Quito, Ecuador<sup>n</sup> LPC, Université Blaise Pascal, CNRS/IN2P3, Clermont, France<sup>o</sup> LPSC, Université Joseph Fourier Grenoble 1, CNRS/IN2P3, Institut National Polytechnique de Grenoble, Grenoble, France<sup>p</sup> CPPM, Aix-Marseille Université, CNRS/IN2P3, Marseille, France<sup>q</sup> LAL, Université Paris-Sud, CNRS/IN2P3, Orsay, France<sup>r</sup> LPNHE, Universités Paris VI and VII, CNRS/IN2P3, Paris, France<sup>s</sup> CEA, Ifrj, SPP, Saclay, France<sup>t</sup> IPHC, Université de Strasbourg, CNRS/IN2P3, Strasbourg, France<sup>u</sup> IPNL, Université Lyon 1, CNRS/IN2P3, Villeurbanne, France<sup>v</sup> Université de Lyon, Lyon, France<sup>w</sup> III. Physikalisches Institut A, RWTH Aachen University, Aachen, Germany<sup>x</sup> Physikalisches Institut, Universität Freiburg, Freiburg, Germany<sup>y</sup> II. Physikalisches Institut, Georg-August-Universität Göttingen, Göttingen, Germany<sup>z</sup> Institut für Physik, Universität Mainz, Mainz, Germany<sup>aa</sup> Ludwig-Maximilians-Universität München, München, Germany<sup>ab</sup> Fachbereich Physik, Bergische Universität Wuppertal, Wuppertal, Germany<sup>ac</sup> Panjab University, Chandigarh, India<sup>ad</sup> Delhi University, Delhi, India<sup>ae</sup> Tata Institute of Fundamental Research, Mumbai, India<sup>af</sup> University College Dublin, Dublin, Ireland<sup>ag</sup> Korea Detector Laboratory, Korea University, Seoul, Republic of Korea<sup>ah</sup> CINVESTAV, Mexico City, Mexico<sup>ai</sup> FOM-Institute NIKHEF and University of Amsterdam/NIKHEF, Amsterdam, The Netherlands<sup>aj</sup> Radboud University Nijmegen/NIKHEF, Nijmegen, The Netherlands<sup>ak</sup> Joint Institute for Nuclear Research, Dubna, Russia<sup>al</sup> Institute for Theoretical and Experimental Physics, Moscow, Russia<sup>am</sup> Moscow State University, Moscow, Russia<sup>an</sup> Institute for High Energy Physics, Protvino, Russia<sup>ao</sup> Petersburg Nuclear Physics Institute, St. Petersburg, Russia<sup>ap</sup> Stockholm University, Stockholm, Sweden<sup>aq</sup> Uppsala University, Uppsala, Sweden

- <sup>af</sup> Lancaster University, Lancaster LA1 4YB, United Kingdom  
<sup>as</sup> Imperial College London, London SW7 2AZ, United Kingdom  
<sup>at</sup> The University of Manchester, Manchester M13 9PL, United Kingdom  
<sup>au</sup> University of Arizona, Tucson, AZ 85721, USA  
<sup>av</sup> University of California Riverside, Riverside, CA 92521, USA  
<sup>aw</sup> Florida State University, Tallahassee, FL 32306, USA  
<sup>ax</sup> Fermi National Accelerator Laboratory, Batavia, IL 60510, USA  
<sup>ay</sup> University of Illinois at Chicago, Chicago, IL 60607, USA  
<sup>az</sup> Northern Illinois University, DeKalb, IL 60115, USA  
<sup>ba</sup> Northwestern University, Evanston, IL 60208, USA  
<sup>bb</sup> Indiana University, Bloomington, IN 47405, USA  
<sup>bc</sup> Purdue University Calumet, Hammond, IN 46323, USA  
<sup>bd</sup> University of Notre Dame, Notre Dame, IN 46556, USA  
<sup>be</sup> Iowa State University, Ames, IA 50011, USA  
<sup>bf</sup> University of Kansas, Lawrence, KS 66045, USA  
<sup>bg</sup> Kansas State University, Manhattan, KS 66506, USA  
<sup>bh</sup> Louisiana Tech University, Ruston, LA 71272, USA  
<sup>bi</sup> Boston University, Boston, MA 02215, USA  
<sup>bj</sup> Northeastern University, Boston, MA 02115, USA  
<sup>bk</sup> University of Michigan, Ann Arbor, MI 48109, USA  
<sup>bl</sup> Michigan State University, East Lansing, MI 48824, USA  
<sup>bm</sup> University of Mississippi, University, MS 38677, USA  
<sup>bn</sup> University of Nebraska, Lincoln, NE 68588, USA  
<sup>bo</sup> Rutgers University, Piscataway, NJ 08855, USA  
<sup>bp</sup> Princeton University, Princeton, NJ 08544, USA  
<sup>bq</sup> State University of New York, Buffalo, NY 14260, USA  
<sup>br</sup> Columbia University, New York, NY 10027, USA  
<sup>bs</sup> University of Rochester, Rochester, NY 14627, USA  
<sup>bt</sup> State University of New York, Stony Brook, NY 11794, USA  
<sup>bu</sup> Brookhaven National Laboratory, Upton, NY 11973, USA  
<sup>bv</sup> Langston University, Langston, OK 73050, USA  
<sup>bw</sup> University of Oklahoma, Norman, OK 73019, USA  
<sup>bx</sup> Oklahoma State University, Stillwater, OK 74078, USA  
<sup>by</sup> Brown University, Providence, RI 02912, USA  
<sup>bz</sup> University of Texas, Arlington, TX 76019, USA  
<sup>ca</sup> Southern Methodist University, Dallas, TX 75275, USA  
<sup>cb</sup> Rice University, Houston, TX 77005, USA  
<sup>cc</sup> University of Virginia, Charlottesville, VA 22901, USA  
<sup>cd</sup> University of Washington, Seattle, WA 98195, USA

## ARTICLE INFO

## Article history:

Received 4 December 2010  
 Received in revised form 9 February 2011  
 Accepted 10 February 2011  
 Available online 24 February 2011  
 Editor: M. Doser

## Keywords:

Tevatron  
 Standard Model  
 Higgs boson  
 Electroweak symmetry breaking

## ABSTRACT

We present a search for associated production of Higgs and  $W$  bosons in  $p\bar{p}$  collisions at a center of mass energy of  $\sqrt{s} = 1.96$  TeV in  $5.3 \text{ fb}^{-1}$  of integrated luminosity recorded by the D0 experiment. Multivariate analysis techniques are applied to events containing one lepton, an imbalance in transverse energy, and one or two  $b$ -tagged jets to discriminate a potential  $WH$  signal from Standard Model backgrounds. We observe good agreement between data and expected backgrounds, and set an upper limit of 4.5 (at 95% confidence level and for  $m_H = 115$  GeV) on the ratio of the  $WH$  cross section multiplied by the branching fraction of  $H \rightarrow b\bar{b}$  to its Standard Model prediction, which is consistent with an expected limit of 4.8.

© 2011 Elsevier B.V. Open access under [CC BY license](#).

The only unobserved particle of the Standard Model (SM) is the Higgs boson ( $H$ ). Its observation would support the hypothesis that the Higgs mechanism generates the masses of the weak gauge bosons and accommodates finite masses of fermions through their Yukawa couplings to the Higgs field. The mass of the Higgs boson ( $m_H$ ) is not predicted by the SM, but the combination of direct searches at the CERN  $e^+e^-$  Collider (LEP) [1] and precision measurements of electroweak parameters constrain  $m_H$  to

$114.4 < m_H < 185$  GeV at the 95% CL [2]. While the region  $158 < m_H < 175$  GeV has been excluded at the 95% CL by a combination of searches at CDF and D0 [3–6], the remaining mass range continues to be probed at the Fermilab Tevatron Collider. The associated production of a Higgs boson and a leptonically-decaying  $W$  boson is among the cleanest Higgs boson search channels at the Tevatron, and provides the largest usable event yield for the decay  $H \rightarrow b\bar{b}$  in the range  $m_H < 135$  GeV. Several searches for  $WH$  production at a  $p\bar{p}$  center-of-mass energy of  $\sqrt{s} = 1.96$  TeV have been published. Three of these [7–9] use subsamples ( $0.17 \text{ fb}^{-1}$ ,  $0.44 \text{ fb}^{-1}$ , and  $1.1 \text{ fb}^{-1}$ ) of the data analyzed in this Letter, while three from the CDF Collaboration are based on cumulative samples ( $0.32 \text{ fb}^{-1}$ ,  $0.95 \text{ fb}^{-1}$  and  $2.7 \text{ fb}^{-1}$ ) of integrated luminosities [10–12].

We present a new search using an improved multivariate technique, in  $5.3 \text{ fb}^{-1}$  of integrated luminosity collected by the D0

<sup>1</sup> Visitor from Augustana College, Sioux Falls, SD, USA.

<sup>2</sup> Visitor from The University of Liverpool, Liverpool, UK.

<sup>3</sup> Visitor from SLAC, Menlo Park, CA, USA.

<sup>4</sup> Visitor from ICREA/IFAE, Barcelona, Spain.

<sup>5</sup> Visitor from Centro de Investigacion en Computacion – IPN, Mexico City, Mexico.

<sup>6</sup> Visitor from ECFM, Universidad Autonoma de Sinaloa, Culiacán, Mexico.

<sup>7</sup> Visitor from Universität Bern, Bern, Switzerland.

detector. The search selects events with one charged lepton ( $\ell =$  electron,  $e$ , or muon,  $\mu$ ), an imbalance in transverse energy ( $\cancel{E}_T$ ) that arises from the unobserved neutrino in the  $W \rightarrow \ell\nu$  decay, and either two or three jets, with one or two of these selected as candidate  $b$ -quark jets ( $b$ -tagged).

The channels are separated into independent categories based on the number of  $b$ -tagged jets in an event (one or two). Single  $b$ -tagged events contain three important sources of backgrounds: (i) multijet events, where a jet is misidentified as an isolated lepton, (ii)  $W$  boson production in association with  $c$ -quark or light-quark jets, and (iii)  $W$  boson production in association with two heavy-flavor ( $b\bar{b}, c\bar{c}$ ) jets. In events with two  $b$ -tagged jets, the dominant backgrounds are from  $Wb\bar{b}$ ,  $t\bar{t}$ , and single top-quark production.

The analysis relies on the following components of the D0 detector [13]: (i) a central-tracking system, which consists of a silicon microstrip tracker (SMT) and a central fiber tracker (CFT), both located within a 2 T superconducting solenoidal magnet; (ii) a liquid-argon/uranium calorimeter containing electromagnetic, fine hadronic, and coarse hadronic layers, segmented into a central section (CC), covering pseudorapidity  $|\eta| < 1.1$  relative to the center of the detector [14], and two end calorimeters (EC) extending coverage to  $|\eta| \approx 4.0$ , all housed in separate cryostats [15], with scintillators between the CC and EC cryostats providing sampling of developing showers for  $1.1 < |\eta| < 1.4$ ; (iii) a muon system located beyond the calorimetry consisting of layers of tracking detectors and scintillation trigger counters, one before and two after the 1.8 T iron toroids. A 2006 upgrade of the D0 detector added an inner layer of silicon [16] to the SMT and an improved calorimeter trigger [17]. The integrated luminosity is measured using plastic scintillator arrays located in front of the EC cryostats at  $2.7 < |\eta| < 4.4$ . The trigger and data acquisition systems are designed to accommodate high instantaneous luminosities.

Events in the electron channel are triggered by a logical OR of several triggers that require an electromagnetic (EM) object or an EM object in conjunction with a jet. Trigger efficiencies are taken into account in the Monte Carlo (MC) simulation through a weighting of events based on an efficiency derived from data, and parametrized as a function of electron  $\eta$  and azimuth  $\phi$ , and jet transverse momentum  $p_T$ .

We accept events for the muon channel from an inclusive mixture of single high- $p_T$  muon, jet and muon plus jet triggers. This inclusive trigger approach provides a gain in efficiency relative to the single muon triggers alone. We validate it by comparing events passed by the single muon triggers and find good agreement between data and MC. Events not selected by the single muon trigger are selected by complementary triggers, typically jet triggers. The efficiency of the complementary triggers is modeled as a function of the scalar sum of the  $p_T$  of jets ( $H_T$ ) in an event, and is used to weight the MC. We find good agreement between data and MC when combining the single muon and complementary triggers to form the inclusive trigger set.

The leading-order (LO) PYTHIA [18] MC generator is used to simulate production of dibosons ( $WW$ ,  $WZ$ , and  $ZZ$ ) with inclusive decays,  $WH \rightarrow l\nu b\bar{b}$  and  $ZH \rightarrow llb\bar{b}$  ( $l = e, \mu, \text{ or } \tau$ ). The contribution from  $ZH$  events (in which one lepton is not identified) to the total signal corresponds to approximately 5%. Background from  $W/Z$  ( $V$ ) + jets and  $t\bar{t}$  events is generated with ALPGEN [19], interfaced to PYTHIA for parton showering and hadronization. The ALPGEN samples are produced in the leading logarithm approximation with the MLM parton-jet matching prescription [19]. The  $V$  + jets samples are divided into  $V$  + light jets and  $V$  + heavy-flavor jets. The  $V$  + light jets samples include  $Vjj$ ,  $Vbj$ , and  $Vcj$  processes, where  $j$  is a light-flavor ( $u, d$  or  $s$  quark or a gluon) jet,

while the  $V$  + heavy-flavor samples for  $Vb\bar{b}$  and  $Vc\bar{c}$  are generated separately. Single top-quark events are generated using COMPHEP [20,21] at next-to-leading order (NLO), with PYTHIA used for parton evolution and hadronization. Simulation of both background and signal processes relies on the CTEQ6L1 [22] LO parton distribution functions for all MC events. These events are processed through the full D0 detector simulation based on GEANT [23], and use the same reconstruction software as used for D0 data. Events from randomly chosen beam crossings with the same instantaneous luminosity profile as the data are overlaid on the simulated events to reproduce the effect of multiple  $p\bar{p}$  interactions and detector noise.

The simulated background processes are normalized to their predicted SM cross sections, except for  $W$  + jets events, which are normalized to data before applying  $b$ -tagging, where contamination from any  $WH$  signal is expected to be negligible. The  $Wb\bar{b}$  ( $Wc\bar{c}$ ) fraction within  $W$  + jets predicted by ALPGEN is increased by the  $K_{b\bar{b}}/K_{l\bar{p}}$  ( $K_{c\bar{c}}/K_{l\bar{p}}$ ) factor, where  $K_{b\bar{b}}$  ( $K_{c\bar{c}}$ ) is the NLO/LO  $K$ -factor for  $Wb\bar{b}$  ( $Wc\bar{c}$ ) and  $K_{l\bar{p}}$  is the NLO/LO  $K$ -factor for  $W$  + (two light partons), as calculated with the MCFM program [24]. The signal cross sections and branching fractions are calculated at next-to-next-to-leading order (NNLO) and are taken from Refs. [25–29], while the  $t\bar{t}$ , single  $t$ , and diboson cross sections are at NLO, and taken from Refs. [30,31], and the MCFM program, respectively. As a cross check, we compare data with the ALPGEN prediction for  $W$  + jets, corrected in such a way that the inclusive  $W$  production cross section is equal to its NNLO calculation [32] with MRST2004 NNLO PDFs [33], and we find a relative data/MC normalization factor of  $1.0 \pm 0.1$  for  $W$  (at least two jets), where all background contributions other than  $W$  + jets were first subtracted from data. Based on the fractions of data events with 0, 1, or 2  $b$ -tagged jets [34], we also observe good agreement with our prediction for the fraction of  $Wb\bar{b}$  and  $Wc\bar{c}$  in  $W$  + jets.

This analysis is based on a preselection of events with an electron of  $p_T > 15$  GeV, with  $|\eta| < 1.1$  or  $1.5 < |\eta| < 2.5$ , or a muon of  $p_T > 15$  GeV, with  $|\eta| < 1.6$ . Preselected events are also required to have  $\cancel{E}_T > 20$  GeV, either two or three jets with  $p_T > 20$  GeV (after correcting jet energies [35]) and  $|\eta| < 2.5$ , and  $H_T > 60$  GeV for 2-jet events, or  $H_T > 80$  GeV for 3-jet events. The  $\cancel{E}_T$  is calculated from the individual calorimeter cells in the EM and fine hadronic layers of the calorimeter, and is corrected for the presence of muons. All energy corrections to electrons and jets (including energy in the coarse-hadronic layers associated with jets) are propagated into the  $\cancel{E}_T$ . To suppress multijet background, events with  $M_T^W < 40 - 0.5\cancel{E}_T$  (GeV) are removed, where  $M_T^W = \sqrt{2E_T^\ell \cdot \cancel{E}_T (1 - \cos\phi(\ell, \cancel{E}_T))}$  is the transverse mass of the  $W$  boson candidate. Events that contain additional charged leptons isolated from jets, with the lepton passing the flavor-dependent  $p_T$  thresholds  $p_T^e > 15$  GeV,  $p_T^\mu > 10$  GeV, and  $p_T^\tau > 10$  or 15 GeV depending on  $\tau$  decay channel [36], are rejected to decrease dilepton background from  $Z$  boson and  $t\bar{t}$  events. Events must have a reconstructed  $p\bar{p}$  interaction vertex (containing at least three associated tracks) that is located within  $\pm 40$  cm of the center of the detector in the longitudinal direction.

Lepton candidates are identified in two steps. First, each candidate must pass “loose” identification criteria. For electrons, we require 95% of the energy in a shower to be deposited in the EM section of the calorimeter (isolation from other calorimeter energy depositions), spatial distributions of calorimeter energies consistent with those expected for EM showers, and a reconstructed track matched to the EM shower, but isolated from other tracks. A “loose” muon is defined by hits in each layer of the muon system, scintillator hits in time with a beam crossing (to veto cosmic

rays), a spatial match with a track in the central tracker, and isolation relative to jet axes ( $\Delta\mathcal{R} > 0.5$ ) [14] to reject semileptonic decays of hadrons. In the second step, the loose leptons are subjected to a more restrictive “tight” selection. Tight electrons must satisfy more restrictive calorimeter isolation and EM energy-fraction criteria, and satisfy a likelihood test developed on  $Z \rightarrow ee$  data based on eight quantities characterizing the EM nature of different particle interactions [37]. Tight muons must satisfy more strict isolation criteria on energy in the calorimeter and on momenta of tracks near trajectories of muon candidates. Inefficiencies introduced by lepton-identification and isolation criteria are determined from  $Z \rightarrow \ell\ell$  data. The final selections for signal rely on events with only tight leptons, and events with loose leptons but not tight leptons are used to determine the multijet background.

Jets are reconstructed using a midpoint cone algorithm [38] with radius 0.5. Identification requirements for jets are based on longitudinal and transverse shower profiles, and minimize the possibility that the jets are caused by noise or spurious depositions of energy. For data taken after the upgrade in 2006, we require that jets in data and in the corresponding simulation have at least two associated tracks emanating from the reconstructed  $p\bar{p}$  interaction vertex. The parameters for jet-identification efficiency, energy calibration, and energy resolution are adjusted accordingly in the simulation to match the data. Also, comparison of ALPGEN with other generators and with data shows small discrepancies in distributions of jet pseudorapidity and dijet angular separations [39]. The data are therefore used to correct the ALPGEN  $W$  + jets and  $Z$  + jets MC events through polynomial reweighting functions, parameterized by the leading and second-leading jet  $\eta$ , and  $\Delta\mathcal{R}$  between the two jets of highest  $p_T$ , that bring these distributions for the total simulated background and in the high-statistics sample of events prior to  $b$ -tagging into agreement.

Instrumental background and that from semileptonic decays of hadrons, referred to jointly as the multijet background, are estimated from data. The instrumental background is significant in the electron channel, where a jet with a high EM fraction can pass electron-identification criteria, or a photon can be misidentified as an electron. In the muon channel, the multijet background is less important and arises mainly from semileptonic decay of heavy-flavor quarks, where the muon passes isolation criteria.

To estimate the number of events that contain a jet that passes “tight” lepton selection, we determine the probability  $f_{T|L}$  for a “loose” lepton candidate, originating from a jet, to also pass tight identification. This is done in events that pass preselection requirements before applying the selection on  $M_T^W$ , i.e., events that contain one loose lepton and two jets, but small  $\cancel{E}_T$  (5–15 GeV). The total non-multijet background is estimated from MC and subtracted from the data before estimating the contribution from multijet events. For electrons,  $f_{T|L}$  is determined as a function of electron  $p_T$  in three regions of  $|\eta|$  and four of  $\Delta\phi(\cancel{E}_T, e)$ , while for muons it is taken as a function of  $|\eta|$  for two regions of  $\Delta\phi(\cancel{E}_T, \mu)$ . The efficiency for a loose lepton to pass the tight identification ( $\varepsilon_{T|L}$ ) is measured in  $Z \rightarrow \ell\ell$  events in data, and is modeled as a function of  $p_T$  for electrons and muons. The estimation of multijet background described in Ref. [37] is used to determine the multijet background directly from data, where each event is assigned a weight that contributes to the multijet estimation based on  $f_{T|L}$  and  $\varepsilon_{T|L}$  as a function of event kinematics. Since  $f_{T|L}$  depends on  $\cancel{E}_T$ , the scale of this estimate of the multijet background must be adjusted when comparing to data with  $\cancel{E}_T > 20$  GeV. Before applying  $b$ -tagging, we fit the background templates to the data  $M_T^W$  distribution to obtain the normalizations for the multijet and  $W$  + jets backgrounds simultaneously.

Efficient identification of  $b$  jets is central to the search for  $WH$  production. The D0 neural network (NN)  $b$ -tagging algorithm [40]

**Table 1**

Summary of event yields for the  $\ell + b$ -tagged jets +  $\cancel{E}_T$  final state. Event yields in data are compared with the expected number of ST and DT events in the samples with  $W$  boson candidates plus two or three jets, comprised of contributions from simulated diboson pairs (labeled “ $WZ$ ” in the table),  $W/Z + b\bar{b}$  or  $c\bar{c}$  (“ $Wb\bar{b}$ ”),  $W/Z$  + light-quark jets (“ $W + lf$ ”), and top-quark (“ $t\bar{t}$ ” and “Single  $t$ ”) production, as well as data-derived multijet background (“MJ”). The quoted uncertainties include both statistical and systematic contributions, including correlations between background sources and channels. The expectation for  $WH$  signal is given for  $m_H = 115$  GeV.

	$W + 2$ -jet ST	$W + 2$ -jet DT	$W + 3$ -jet ST	$W + 3$ -jet DT
$WZ$	$153 \pm 18$	$22.5 \pm 3.3$	$33.9 \pm 4.8$	$2.6 \pm 1.1$
$Wb\bar{b}$	$1601 \pm 383$	$346 \pm 93$	$358 \pm 90$	$48 \pm 13$
$W + lf$	$1290 \pm 201$	$57.5 \pm 9.2$	$210 \pm 35$	$12.1 \pm 1.8$
$t\bar{t}$	$417 \pm 54$	$177 \pm 35$	$633 \pm 96$	$176 \pm 35$
Single $t$	$203 \pm 33$	$58 \pm 11$	$53.6 \pm 9.1$	$13.0 \pm 2.7$
MJ	$663 \pm 43$	$56.5 \pm 4.2$	$186 \pm 13$	$12.7 \pm 1.0$
All Bkg.	$4326 \pm 501$	$718 \pm 120$	$1474 \pm 160$	$264 \pm 44$
$WH$	$9.7 \pm 0.9$	$6.5 \pm 1.0$	$2.1 \pm 0.3$	$0.8 \pm 0.2$
Data	4316	709	1463	301

for identifying heavy-flavored jets is based on a combination of seven variables sensitive to the presence of tracks or secondary vertices displaced significantly from the primary vertex. All tagging efficiencies are determined separately for data and for simulated events. We first use a low threshold on the NN output that corresponds to a rate of 2.7% for light-flavor jets of  $p_T \geq 50$  GeV that are mistakenly tagged as heavy-flavored jets. If two jets in an event pass this  $b$ -tagging requirement, the event is classified as double- $b$ -tagged (DT). Events that are not classified as DT are considered for placement in an independent single- $b$ -tag (ST) sample, which requires exactly one jet to satisfy a more restrictive NN operating point corresponding to a misidentification rate of 0.9%. The efficiencies for identifying a jet that contains a  $b$  hadron for the two NN operating points are  $(63 \pm 1)\%$  and  $(53 \pm 1)\%$ , respectively, for a jet with a  $p_T$  of 50 GeV. These efficiencies are determined for “taggable” jets, i.e., jets with at least two tracks, each with at least one hit in the SMT. Simulated events are corrected to have the same fraction of jets satisfying the taggability and  $b$ -tagging requirements as found in preselected data.

The expected event yields following these selection criteria for specific backgrounds and for  $m_H = 115$  GeV are compared to the observed number of events in Table 1. Distributions in dijet invariant mass for the two jets of highest  $p_T$ , in 2-jet and 3-jet events are shown for the ST and DT samples in Figs. 1(a)–1(d). The data are adequately described by the sum of the simulated SM processes and multijet background. The contributions expected from a Higgs boson with  $m_H = 115$  GeV, multiplied by a factor of ten, are also shown for comparison.

We use a random forest (RF) multivariate technique [41,42] to separate the SM background from signal, and search for an excess, which is expected primarily at large values of RF discriminant. A separate RF discriminant is used for each combination of jet multiplicity (two or three), lepton flavor ( $e$  or  $\mu$ ), and number of  $b$ -tagged jets (one or two). The 2-jet events are divided into data-taking periods, before and after the 2006 detector upgrade, for a total of twelve separately trained RFs for each chosen Higgs boson mass. Each RF consists of a collection of individual decision trees, with each tree considering a random subset of the twenty kinematic and topological input variables listed in Table 2. The final RF output is the average over the individual trees. The input variables  $\sqrt{s}$  and  $\Delta\mathcal{R}(\text{dijet}, \ell + \nu)$  each have two solutions arising from the two possibilities for the longitudinal neutrino momentum, assuming the lepton and  $\cancel{E}_T$  ( $\nu$ ) constitute the decay products of an on-shell  $W$  boson. The angles  $\theta^*$  and  $\chi$  are described in Ref. [43], and exploit kinematic differences arising from the scalar nature of

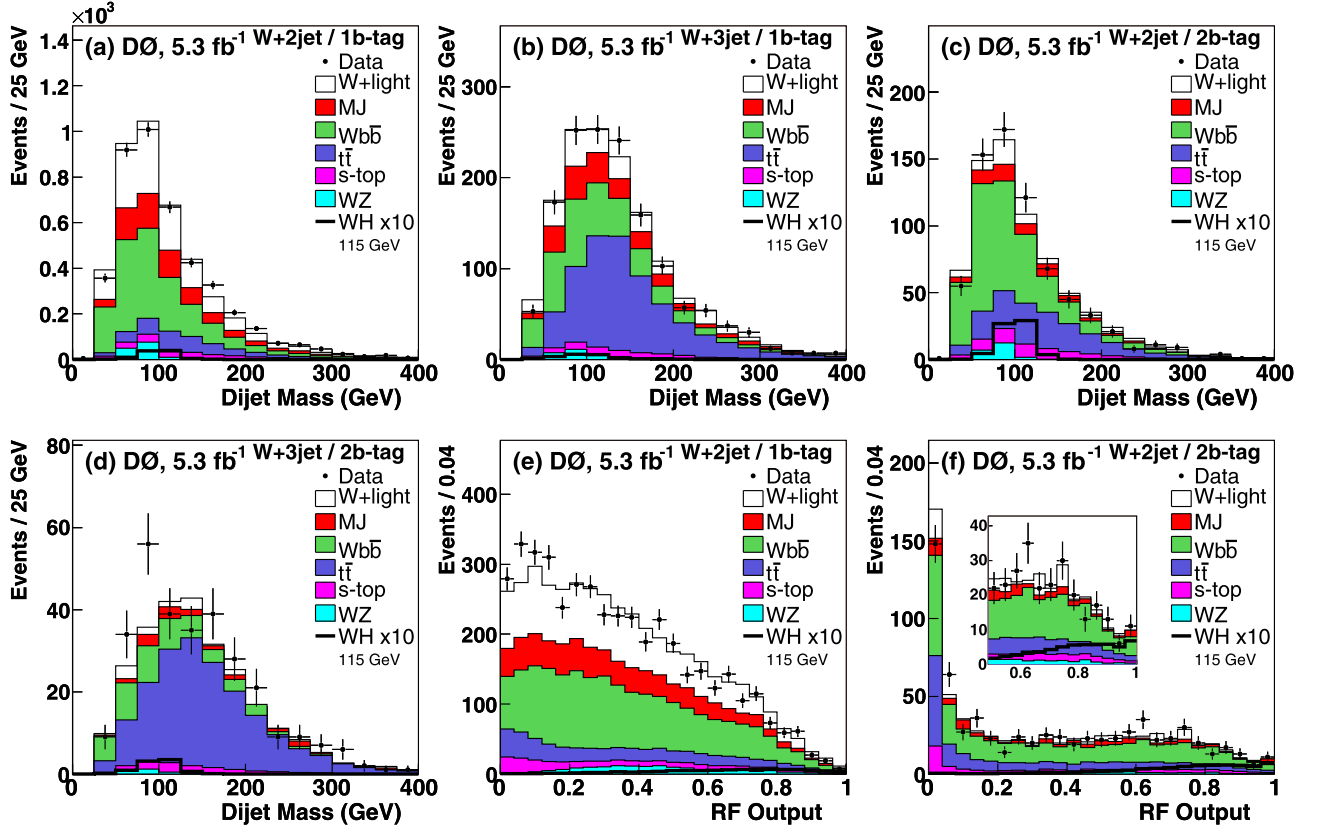


**Fig. 1.** (Color online.) Dijet mass distributions for candidate  $W$ -boson ST (1  $b$ -tag) events with (a) 2-jets and (b) 3-jets and for DT (2  $b$ -tag) events in (c) and (d), respectively. The distributions in RF discriminant for 2-jet ST and DT events, combined for lepton flavors, are shown in (e) and (f), respectively. The expectation from  $\sigma(p\bar{p} \rightarrow WH) \times \mathcal{B}(H \rightarrow b\bar{b})$  for  $m_H = 115$  GeV is overlaid, multiplied by a factor of 10.

**Table 2**

List of RF input variables, where  $j_1$  ( $j_2$ ) refers to the jet with the highest (second highest)  $p_T$ .

Variable	Definition
$p_T(j_1)$	Leading jet $p_T$
$p_T(j_2)$	Sub-leading jet $p_T$
$E(j_2)$	Sub-leading jet energy
$\Delta\mathcal{R}(j_1, j_2)$	$\Delta\mathcal{R}$ between jets
$\Delta\phi(j_1, j_2)$	$\Delta\phi$ between jets
$\Delta\phi(j_1, \ell)$	$\Delta\phi$ between lepton and leading jet
$p_T(\text{dijet system})$	$p_T$ of dijet system
$m_{jj}$	Dijet invariant mass
$p_T(\ell - \cancel{E}_T \text{ system})$	$p_T$ of $W$ candidate
$\cancel{E}_T$	Missing transverse energy
Aplanarity	See Ref. [44]
$\sqrt{s}$	Invariant mass of the $\nu + \ell + \text{dijet system}$
$\Delta\mathcal{R}(\text{dijet}, \ell + \nu)$	$\Delta\mathcal{R}$ between the dijet system and $\ell + \nu$ system
$M_T^W$	Lepton- $\cancel{E}_T$ transverse mass
$H_T$	Scalar sum of the transverse momenta of all jets in the event
$H_Z$	Scalar sum of the longitudinal momenta of all jets in the event
$\cos\theta^*$	Cosine of angle between $W$ candidate and beam direction in zero-momentum frame
$\cos\chi$	See Ref. [45]

the Higgs and the spins of objects in the  $Wb\bar{b}$  background. The RF outputs from 2-jet ST and DT events are shown in Figs. 1(e) and 1(f).

The dijet mass distribution is especially sensitive to  $WH$  production, and was used previously to set limits on  $\sigma(p\bar{p} \rightarrow WH) \times \mathcal{B}(H \rightarrow b\bar{b})$  in Ref. [8]. However, the gain in sensitivity using the

RF output as the final discriminant is about 20% for a Higgs mass of 115 GeV, which, in terms of the expected limit on the  $WH$  cross section, is equivalent to a gain of about 40% in integrated luminosity.

The systematic uncertainties that affect the signal and SM backgrounds can be categorized by the nature of their source, i.e., theoretical (e.g., uncertainty on a cross section), MC modeling (e.g., reweighting of ALPGEN samples), or experimental (e.g., uncertainty on integrated luminosity). Some of these uncertainties affect only the normalization of the signal or backgrounds, while others also affect the differential distribution of the RF output.

Theoretical uncertainties include uncertainties on the  $t\bar{t}$  and single top-quark production cross sections (10% and 12%, respectively [30,31]), an uncertainty on the diboson production cross section (6% [24]), and an uncertainty on  $W + \text{heavy-flavor production}$  (20%, estimated from MCFM). These uncertainties affect only the normalization of the backgrounds.

Uncertainties from modeling that affect the distribution in the RF output include uncertainties on trigger efficiency as derived from data (3–5%), lepton identification and reconstruction efficiency (5–6%), reweighting of ALPGEN MC samples (2%), the MLM matching applied to  $W/Z + \text{light-jet events}$  (<0.5%), and the systematic uncertainties associated with choice of renormalization and factorization scales in ALPGEN as well as the uncertainty on the strong coupling constant (2%). Uncertainties on the ALPGEN renormalization and factorization scales are evaluated by adjusting the nominal scale for each, simultaneously, by a factor of 0.5 and 2.0.

Experimental uncertainties that affect only the normalization of the signal and SM backgrounds arise from the uncertainty on

**Table 3**Expected and observed 95% CL upper limits on the ratio of  $\sigma(p\bar{p} \rightarrow WH) \times \mathcal{B}(H \rightarrow b\bar{b})$  to its SM expectation as a function of  $m_H$ .

$m_H$ [GeV]	100	105	110	115	120	125	130	135	140	145	150
Expected ratio	3.3	3.6	4.2	4.8	5.6	6.8	8.5	11.5	16.5	23.6	36.8
Observed ratio	2.7	4.0	4.3	4.5	5.8	6.6	7.0	7.6	12.2	15.0	30.4

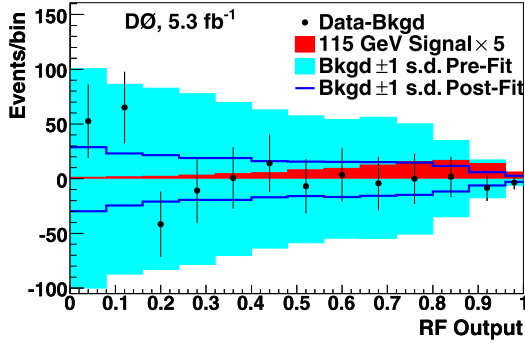


**Fig. 2.** (Color online.) Distribution in the output of the RF discriminant for  $m_H = 115$  GeV, for the difference between data and background expectation, combined for all channels (both  $e$  and  $\mu$ , ST and DT, and 2-jet and 3-jet), shown with statistical uncertainties. The lightly-shaded region represents the total systematic uncertainty before using constraints from data (referred to as “Pre-Fit” in the legend), while the solid lines represent the total systematic uncertainty after constraining with data (“Post-Fit” in the legend). The darker shaded region represents the SM Higgs signal expectation scaled up by a factor of 5.

integrated luminosity (6.1%) [46]. Those that also affect the distribution in RF output include jet taggability (3%),  $b$ -tagging efficiency (2.5–3% per heavy quark-jet), the light-quark jet misidentification rate (10%), acceptance for jet identification (5%); jet-energy calibration and resolution (varies between 15% and 30%, depending on the process and channel). Model in multijet background is limited by the statistical uncertainty of data after tagging (10–20%), which also covers the uncertainty in the flavor dependence of  $f_{T|L}$ . The background-subtracted data points for the RF discriminant for  $m_H = 115$  GeV, with all channels combined, are shown with their systematic uncertainties in Fig. 2.

We observe no excess relative to expectation from SM background, and we set upper limits on the production cross section  $\sigma(WH)$  using the RF outputs from all the channels. The binning of the RF output is adjusted to assure adequate population of background events in each bin. We calculate all limits at the 95% CL using a modified frequentist approach and a Poisson log-likelihood ratio as test statistic [47,48]. The likelihood ratio is studied using pseudoexperiments based on randomly drawn Poisson trials of signal and background events. We treat systematic uncertainties as “nuisance parameters” constrained by their priors, and the best fits of these parameters to data are determined at each value of  $m_H$  by maximizing the likelihood ratio [49]. Independent fits are performed to the background-only and signal-plus-background hypotheses. All appropriate correlations of systematic uncertainties are maintained among channels and between signal and background. The systematic uncertainties before and after fitting are indicated in Fig. 2. The log-likelihood ratios for the background-only model and the signal-plus-background model as a function of  $m_H$  are shown in Fig. 3(a).

The upper limit on  $\sigma(p\bar{p} \rightarrow WH) \times \mathcal{B}(H \rightarrow b\bar{b})$  at the 95% CL is a factor of 4.5 larger than the SM expectation for  $m_H = 115$  GeV, and the corresponding expected upper limit is 4.8. The analysis is repeated for ten other  $m_H$  values from 100 to 150 GeV; the corresponding observed and expected 95% CL limits relative to their SM expectations are given in Table 3 and in Fig. 3(b).

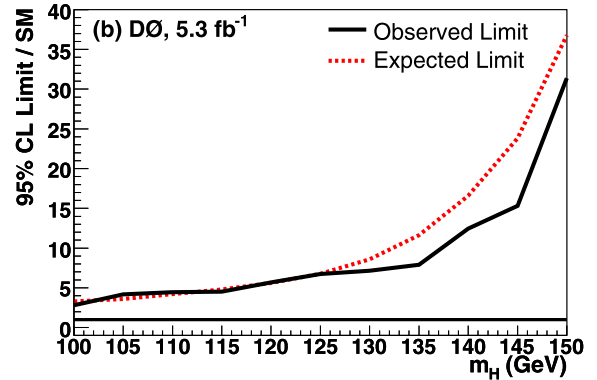
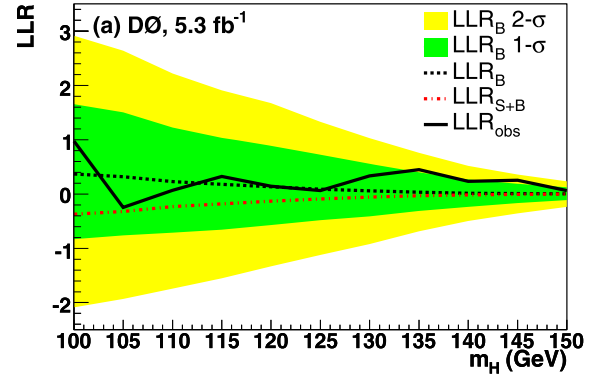


**Fig. 3.** (Color online.) (a) Log-likelihood ratios for the background-only model ( $LLR_B$ , with 1 and 2 standard deviation bands), signal + background model ( $LLR_{S+B}$ ), and observation in data ( $LLR_{obs}$ ) as a function of  $m_H$ . (b) 95% CL cross section upper limit (and the corresponding expected limit) on  $\sigma(p\bar{p} \rightarrow WH) \times \mathcal{B}(H \rightarrow b\bar{b})$  relative to the SM expectation, as a function of  $m_H$ . Results are calculated in steps of 5 GeV, and joined by straight lines.

In conclusion,  $\ell + \cancel{E}_T + 2$  or 3-jet events have been analyzed in a search for  $WH$  production in  $5.3 \text{ fb}^{-1}$  of  $p\bar{p}$  collisions at the Fermilab Tevatron. The yield of single and double  $b$ -tagged jets in these events is in agreement with the expected background. We have applied a Random Forest multivariate analysis technique to further separate signal and background. We have set upper limits on  $\sigma(p\bar{p} \rightarrow WH) \times \mathcal{B}(H \rightarrow b\bar{b})$  relative to their SM expectation for Higgs masses between 100 and 150 GeV. For  $m_H = 115$  GeV, the observed (expected) 95% CL limit is a factor of 4.5 (4.8) larger than the SM expectation.

### Acknowledgements

We thank the staffs at Fermilab and collaborating institutions, and acknowledge support from the DOE and NSF (USA); CEA and CNRS/IN2P3 (France); FASI, Rosatom and RFBR (Russia); CNPq, FAPERJ, FAPESP and FUNDUNESP (Brazil); DAE and DST (India); Colciencias (Colombia); CONACyT (Mexico); KRF and KOSEF (Korea); CONICET and UBACyT (Argentina); FOM (The Netherlands); STFC and the Royal Society (United Kingdom); MSMT and GACR (Czech Republic); CRC Program and NSERC (Canada); BMBF and DFG (Germany); SFI (Ireland); The Swedish Research Council (Sweden); and CAS and CNSF (China).

## References

- [1] ALEPH Collaboration, DELPHI Collaboration, L3 Collaboration, OPAL Collaboration, LEP Working Group for Higgs Boson Searches, Phys. Lett. B 565 (2003) 61.
- [2] LEP Electroweak Working Group, <http://lepewwg.web.cern.ch/LEPEWWG/>.
- [3] T. Aaltonen, et al., CDF Collaboration, Phys. Rev. Lett. 104 (2010) 061803.
- [4] V.M. Abazov, et al., D0 Collaboration, Phys. Rev. Lett. 104 (2010) 061804.
- [5] T. Aaltonen, et al., CDF Collaboration, D0 Collaboration, Phys. Rev. Lett. 104 (2010) 061802.
- [6] T. Aaltonen, et al., CDF Collaboration, D0 Collaboration, FERMILAB-CONF-10-257-E, 2010.
- [7] V.M. Abazov, et al., D0 Collaboration, Phys. Rev. Lett. 94 (2005) 091802.
- [8] V.M. Abazov, et al., D0 Collaboration, Phys. Lett. B 663 (2008) 26.
- [9] V.M. Abazov, et al., D0 Collaboration, Phys. Rev. Lett. 102 (2009) 051803.
- [10] D. Acosta, et al., CDF Collaboration, Phys. Rev. Lett. 94 (2005) 091802.
- [11] T. Aaltonen, et al., CDF Collaboration, Phys. Rev. Lett. 100 (2008) 041801.
- [12] T. Aaltonen, et al., CDF Collaboration, Phys. Rev. Lett. 103 (2009) 101802.
- [13] V.M. Abazov, et al., D0 Collaboration, Nucl. Instrum. Methods Phys. Res. A 565 (2006) 463.
- [14] Pseudorapidity  $\eta = -\ln[\tan \frac{\theta}{2}]$ , where  $\theta$  is the polar angle as measured from the beam axis;  $\phi$  is the azimuthal angle. The separation between two objects in  $\eta, \phi$  space is  $\Delta\mathcal{R} = \sqrt{(\Delta\eta)^2 + (\Delta\phi)^2}$ .
- [15] S. Abachi, et al., Nucl. Instrum. Methods Phys. Res. A 338 (1994) 185.
- [16] R. Angstadt, et al., Nucl. Instrum. Methods Phys. Res. A 622 (2010) 298.
- [17] M. Abolins, et al., Nucl. Instrum. Methods Phys. Res. A 584 (2008) 75.
- [18] T. Sjöstrand, S. Mrenna, P. Skands, J. High Energy Phys. 0605 (2006) 026, versions 6.319, 6.323 and 6.409. Tune A was used.
- [19] M. Mangano, et al., J. High Energy Phys. 0307 (2003) 001, version 2.05.
- [20] A. Pukhov, et al., hep-ph/9908288, 1999.
- [21] E. Boos, et al., Nucl. Instrum. Methods Phys. Res. A 534 (2004) 250.
- [22] J. Pumplin, et al., J. High Energy Phys. 0207 (2002) 012.
- [23] R. Brun, F. Carminati, CERN Program Library Long Writeup, report W5013, 1993.
- [24] J.M. Campbell, R.K. Ellis, Phys. Rev. D 60 (1999) 113006.
- [25] K.A. Assamagan, et al., arXiv:hep-ph/0406152.
- [26] O. Brein, A. Djouadi, R. Harlander, Phys. Lett. B 579 (2004) 149.
- [27] M.L. Ciccolini, S. Dittmaier, M. Krämer, Phys. Rev. D 68 (2003) 073003.
- [28] J. Baglio, A. Djouadi, J. High Energy Phys. 1010 (2010) 064.
- [29] A. Djouadi, J. Kalinowski, M. Spira, Comput. Phys. Commun. 108 (1998) 56.
- [30] N. Kidonakis, et al., Phys. Rev. D 78 (2008) 074005.
- [31] N. Kidonakis, Phys. Rev. D 74 (2006) 114012.
- [32] R. Hamberg, W.L. van Neerven, W.B. Kilgore, Nucl. Phys. B 359 (1991) 343; R. Hamberg, W.L. van Neerven, W.B. Kilgore, Nucl. Phys. B 644 (2002) 403.
- [33] A.D. Martin, R.G. Roberts, W.J. Stirling, R.S. Thorne, Phys. Lett. B 604 (2004) 61.
- [34] V.M. Abazov, et al., D0 Collaboration, FERMILAB-PUB-10/544-E, 2010, arXiv:1101.0124 [hep-ex], Phys. Rev. D, submitted for publication.
- [35] J. Hegeman, J. Phys. Conf. Ser. 160 (2009) 012024.
- [36] V.M. Abazov, et al., D0 Collaboration, Phys. Lett. B 670 (2009) 292. Only tau leptons decaying to hadrons are considered as tau candidates; those decaying to electrons or muons are included in the respective lepton contribution.
- [37] V.M. Abazov, et al., D0 Collaboration, Phys. Rev. D 76 (2007) 092007.
- [38] G. Blazey, et al., in: U. Baur, R.K. Ellis, D. Zeppenfeld (Eds.), Proceedings of the Workshop “QCD and Weak Boson Physics in Run II”, 2000, p. 47, arXiv:hep-ex/0005012, Fermilab-Pub-00/297.
- [39] J. Alwall, et al., Eur. Phys. C 53 (2008) 473.
- [40] V.M. Abazov, et al., D0 Collaboration, Nucl. Instrum. Methods Phys. Res. A 620 (2010) 490.
- [41] L. Breiman, Machine Learning 45 (2001) 5.
- [42] I. Narsky, arXiv:physics/0507143, 2005.
- [43] S. Parke, S. Veseli, Phys. Rev. D 60 (1999) 093003.
- [44] Aplanarity is defined as  $\frac{3}{2}\lambda_3$ , where  $\lambda_3$  is the smallest eigenvalue of the normalized momentum tensor  $\mathcal{M}_{ij} = (\sum_o p_i^o p_j^o) / (\sum_o |\vec{p}^o|^2)$ , where  $o$  runs over the jets and charged lepton in the event, and  $p_i^o$  is the  $i$ -th 3-momentum component of the  $o$ -th physics object.
- [45]  $\chi$  is the angle between the charged lepton and dijet system after boosting into the  $W$  boson rest frame and then rotating the dijet system 4-vector as described in Ref. [43].
- [46] T. Andeen, et al., FERMILAB-TM-2365, 2007.
- [47] T. Junk, Nucl. Instrum. Methods Phys. Res. A 434 (1999) 435.
- [48] A. Read, J. Phys. G 28 (2002) 2693.
- [49] W. Fisher, FERMILAB-TM-2386-E, 2007.